Inorganic Chemistry

Article

pubs.acs.org/IC

Mononuclear Gold(I) Acetylide Complexes with Urea Group: Synthesis, Characterization, Photophysics, and Anion Sensing Properties

Yu-Peng Zhou, Mei Zhang, Yu-Hao Li, Qi-Rui Guan, Fang Wang, Zhuo-Jia Lin, Chi-Keung Lam, Xiao-Long Feng, and Hsiu-Yi Chao*

MOE Key Laboratory of Bioinorganic and Synthetic Chemistry, School of Chemistry and Chemical Engineering, Sun Yat-Sen University, Guangzhou 510275, P. R. China

Supporting Information

ABSTRACT: A series of mononuclear gold(I) acetylide complexes with urea moiety, $R'_3PAuC{\equiv}CC_6H_4$-4-$NHC(O)NHC_6H_4$-4-R (R′ = cyclohexyl, R = NO_2 (**2a**), CF_3 (**2b**), Cl (**2c**), H (**2d**), CH_3 (**2e**), ^{t}Bu (**2f**), OCH_3 (**2g**); R′ = phenyl, R = NO_2 (**3a**), OCH_3 (**3b**); R′ = 4-methoxyphenyl, R = H (**4a**), OCH_3 (**4b**)), have been synthesized and characterized. The crystal structures of $Ph_3PAuC{\equiv}CC_6H_4$-4-$NHC(O)NHC_6H_4$-4-NO_2 (**3a**) and $(4\text{-}CH_3OC_6H_4)_3PAuC{\equiv}CC_6H_4$-4-$NHC(O)NHC_6H_5$ (**4a**) have been determined by X-ray diffraction. Complexes **2a**−**2g**, **3b**, and **4a**−**4b** show intense luminescence both in the solid state and in degassed THF solution at 298 K. Anion binding properties of complexes **2a**−**2g**, **3a**−**3b**, and **4a**−**4b** have been studied by UV−vis and ^{1}H NMR titration experiments. In general, the log K values of **2a**−**2g** with the same anion in THF depend on the substituent R on the acetylide ligand of **2a**−**2g**: R = NO_2 (**2a**) > CF_3 (**2b**) ≥ Cl (**2c**) > H (**2d**) > CH_3 (**2e**) ≈ ^{t}Bu (**2f**) ≥ OCH_3 (**2g**). Complex **2a** with NO_2 group shows the dramatic color change toward F^- in DMSO, which provides an access of naked eye detection of F^-.

INTRODUCTION

Since the first anion sensor reported by Park and Simmons in 1968,[1] anion sensors have attracted much attention because of their potential applications in the environment[2] and in biology.[3] For an anion sensor, it usually consists of two main moieties: recognition unit and sensing unit. The recognition unit could interact with anions by noncovalent interactions, such as a hydrophobic effect,[4a] metal or Lewis acid coordination,[4b] electrostatic interactions,[4c] anion−π interactions,[5] halogen bonding,[6] and hydrogen bonding.[7] Various recognition units, for example, thiourea,[7a] urea,[7] amide,[8] and guandinium,[9] have been utilized to interact with anions. Among them, the urea group is one of the most frequently used recognition units because it has unique geometry with two N−H bonds and its modification can be easily carried out by organic synthesis.[7b] Fabbrizzi,[10] Gunnlaugsson,[11] Gale,[12] and other groups[13] have reported the synthesis of various urea-based organic anion sensors.

In addition to an organic anion sensing unit, metal complexes have been used as anion sensors due to their various properties like redox and luminescence, which could provide the various accesses of sensing.[14] The incorporation of ferrocene,[15] ruthenium(II) polypyridyl,[16] terbium(III) cyclen,[17] gold(I) thiolate,[18a,b] or gold(I)−copper(I) acetylide[18c] into the urea moiety has been reported in the literature. Among these metal complexes, gold(I) complexes with d^{10} closed electronic shell and linear geometry are quite important[19] due to their potential use in the area of biology,[20] drugs,[21] catalysis,[22] OLEDs,[23a] and OPL materials.[23b] In addition, utilization of the rich photophysical properties and various geometries of gold(I) complexes as chemosensors has been developed recently.[24]

The acetylide ligands with the structure of unsaturated sp C-atom and strong σ-donating center lead to the rich structure diversity as well as unique optical and electronic properties to the metal complexes,[25] which could provide the potential applications in nonlinear optics, liquid crystals, luminescence, molecule wires, and ion sensors.[18c,24,25a,26−29] Yam and co-workers have synthesized Au(I)−Cu(I) acetylide complexes containing urea group and studied the sensing properties toward anions.[18c] Other metal acetylide complexes, such as platinum(II)[28] and ruthenium(II) acetylide[29] complexes with nonurea moieties, have also been used as the anion sensors.

We have a long-term interest in studying the relationship between the structures and photophysical properties of metal acetylide complexes.[30] To extend our work on the structures and photophysical properties of gold(I) acetylide complexes, in this work, a series of mononuclear gold(I) acetylide complexes

Received: December 5, 2011
Published: April 9, 2012

   dx.doi.org/10.1021/ic202608r | Inorg. Chem. 2012, 51, 5099−5109

Scheme 1. Synthetic Route of Gold(I) Acetylide Complexes 2a−2g, 3a−3b, and 4a−4b

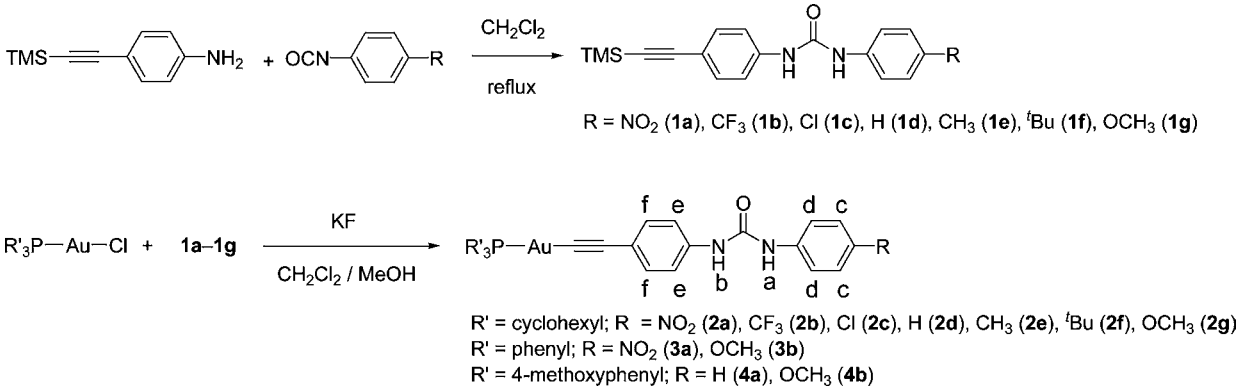

with urea group, $R'_3PAuC{\equiv}CC_6H_4$-4-$NHC(O)NHC_6H_4$-4-R (R′ = cyclohexyl, R = NO_2 (**2a**), CF_3 (**2b**), Cl (**2c**), H (**2d**), CH_3 (**2e**), ^{t}Bu (**2f**), OCH_3 (**2g**); R′ = phenyl, R = NO_2 (**3a**), OCH_3 (**3b**); R′ = 4-methoxyphenyl, R = H (**4a**), OCH_3 (**4b**); Scheme 1), have been synthesized and characterized. The crystal structures of $Ph_3PAuC{\equiv}CC_6H_4$-4-$NHC(O)NHC_6H_4$-4-NO_2 (**3a**) and $(4\text{-}CH_3OC_6H_4)_3PAuC{\equiv}CC_6H_4$-4-$NHC(O)NHC_6H_5$ (**4a**) were determined by X-ray diffraction. We envisaged that if the photophysical properties of these gold(I) acetylide complexes could be changed when they interact with anions through hydrogen bonds between the urea N−H of the complexes and anions, they could be used as anion sensors. The effect of structure, including the substituent R on the acetylide ligand of the complex as well as the auxiliary phosphine ligand, on the binding ability of the gold(I) acetylide complexes with anions has also been studied.

EXPERIMENTAL SECTION

Materials and Reagents. 4-[(Trimethylsilyl)ethynyl]aniline[31] and R'_3PAuCl (R′ = cyclohexyl, phenyl, and 4-methoxyphenyl)[32] were synthesized according to literature procedures. 4-Nitrophenyl isocyanate, *p*-tolyl isocyanate, 4-methoxyphenyl isocyanate, and tetra-*n*-butylammonium phosphate were purchased from Acros. Tetra-*n*-butylammonium fluoride hydrate and tetra-*n*-butylammonium acetate were obtained from Sigma-Aldrich. 4-Chlorophenyl isocyanate, tetra-*n*-butylammonium nitrate, and tetra-*n*-butylammonium chloride hydrate were purchased from Alfa-Aesar. 4-(Trifluoromethyl)phenyl isocyanate, 4-*tert*-butylphenyl isocyanate, and tetra-*n*-butylammonium bromide were obtained from J&K. Phenyl isocyanate was purchased from Aladdin. All reactions were carried out under anhydrous and anaerobic conditions using standard Schlenk techniques under nitrogen.

Synthesis. General procedure for the synthesis of **1a−1g**: To a solution of 4-[(trimethylsilyl)ethynyl]aniline in CH_2Cl_2 was added 1 equiv of the corresponding isocynate in CH_2Cl_2. The mixture was heated to reflux for 24 h. The solvent was removed under reduced pressure, and the residue was washed with *n*-hexane to yield yellow solids.

1a. Yield: 164 mg, 75%. ^{1}H NMR (300 MHz, DMSO-d_6, 298 K): δ = 9.44 (s, 1 H, NH), 9.08 (s, 1 H, NH), 8.15 (d, J = 9 Hz, 2 H, aromatic ring), 7.65 (d, J = 9 Hz, 2 H, aromatic ring), 7.45 (d, J = 9 Hz, 2 H, aromatic ring), 7.35 (d, J = 9 Hz, 2 H, aromatic ring), 0.20 (s, 9 H, $Si(CH_3)_3$). ESI-MS: m/z = 352 $[M - H]^-$. Anal. Calcd for $C_{18}H_{19}N_3O_3Si$ (%): C, 61.17; H, 5.42; N, 11.89. Found: C, 61.10; H, 5.50; N, 11.60.

1b. Yield: 56 mg, 79%. ^{1}H NMR (300 MHz, DMSO-d_6, 298 K): δ = 9.12 (s, 1 H, NH), 8.97 (s, 1 H, NH), 7.59 (m, 4 H, aromatic ring), 7.42 (d, J = 9 Hz, 2 H, aromatic ring), 7.33 (d, J = 9 Hz, 2 H, aromatic ring), 0.19 (s, 9 H, $Si(CH_3)_3$). ^{19}F NMR (228 MHz, DMSO-d_6, 298 K): δ = −60.76 (s). ESI-MS: m/z = 376 $[M - H]^-$. Anal. Calcd for $C_{19}H_{19}F_3N_2OSi$ (%): C, 60.62; H, 5.09; N, 7.44. Found: C, 60.47; H, 5.28; N, 7.34.

1c. Yield: 365 mg, 94%. ^{1}H NMR (300 MHz, DMSO-d_6, 298 K): δ = 8.90 (s, 1 H, NH), 8.86 (s, 1 H, NH), 7.46 (d, J = 7 Hz, 2 H, aromatic ring), 7.43 (d, J = 7 Hz, 2 H, aromatic ring), 7.34 (d, J = 7 Hz, 2 H, aromatic ring), 7.31 (d, J = 7 Hz, 2 H, aromatic ring), 0.21 (s, 9 H, $Si(CH_3)_3$). ESI-MS: m/z = 341 $[M - H]^-$. Anal. Calcd for $C_{18}H_{19}ClN_2OSi$ (%): C, 63.05; H, 5.59; N, 8.17. Found: C, 62.91; H, 5.55; N, 8.13.

1d. Yield: 132 mg, 89%. ^{1}H NMR (300 MHz, DMSO-d_6, 298 K): δ = 8.87 (s, 1 H, NH), 8.72 (s, 1 H, NH), 7.44 (d, J = 8 Hz, 2 H, aromatic ring), 7.41 (d, J = 8 Hz, 2 H, aromatic ring), 7.34 (d, J = 9 Hz, 2 H, aromatic ring), 7.26 (dd, J_1 = 8 Hz, J_2 = 8 Hz, 2 H, aromatic ring), 6.96 (dd, J_1 = 8 Hz, J_2 = 8 Hz, 1 H, aromatic ring), 0.22 (s, 9 H, $Si(CH_3)_3$). ESI-MS: m/z = 308 $[M - H]^-$. Anal. Calcd for $C_{18}H_{20}N_2OSi$ (%): C, 70.09; H, 6.54; N, 9.08. Found: C, 69.81; H, 6.39; N, 9.03.

1e. Yield: 354 mg, 95%. ^{1}H NMR (300 MHz, DMSO-d_6, 298 K): δ = 8.79 (s, 1 H, NH), 8.57 (s, 1 H, NH), 7.42 (d, J = 9 Hz, 2 H, aromatic ring), 7.32 (m, 4 H, aromatic ring), 7.06 (d, J = 8 Hz, 2 H, aromatic ring), 2.23 (s, 3 H, CH_3), 0.21 (s, 9 H, $Si(CH_3)_3$). ESI-MS: m/z = 321 $[M - H]^-$. Anal. Calcd for $C_{19}H_{22}N_2OSi$ (%): C, 70.77; H, 6.88; N, 8.69. Found: C, 70.59; H, 6.84; N, 8.62.

1f. Yield: 379 mg, 92%. ^{1}H NMR (300 MHz, DMSO-d_6, 298 K): δ = 8.81 (s, 1 H, NH), 8.61 (s, 1 H, NH), 7.43 (d, J = 9 Hz, 2 H, aromatic ring), 7.34 (m, 4 H, aromatic ring), 7.27 (d, J = 9 Hz, 2 H, aromatic ring), 1.26 (s, 9 H, $C(CH_3)_3$), 0.22 (s, 9 H, $Si(CH_3)_3$). ESI-MS: m/z = 363 $[M - H]^-$. Anal. Calcd for $C_{22}H_{28}N_2OSi$ (%): C, 72.48; H, 7.74; N, 7.68. Found: C, 72.48; H, 7.74; N, 7.59.

1g. Yield: 123 mg, 78%. ^{1}H NMR (300 MHz, DMSO-d_6, 298 K): δ = 8.80 (s, 1 H, NH), 8.54 (s, 1 H, NH), 7.42 (d, J = 9 Hz, 2 H, aromatic ring), 7.32 (d, J = 9 Hz, 4 H, aromatic ring), 6.85 (d, J = 9 Hz, 2 H, aromatic ring), 3.71 (s, 3 H, OCH_3), 0.22 (s, 9 H, $Si(CH_3)_3$). ESI-MS: m/z = 337 $[M - H]^-$. Anal. Calcd for $C_{19}H_{22}N_2O_2Si$ (%): C, 67.42; H, 6.55; N, 8.28. Found: C, 67.28; H, 6.59; N, 8.30.

General procedure for the synthesis of **2a−2g**, **3a−3b**, and **4a−4b** follows: To a mixture of R'_3PAuCl (R′ = cyclohexyl, phenyl, or 4-methoxyphenyl) and 1 equiv of the corresponding acetylide ligand in CH_2Cl_2 was added 2 equiv of $KF{\cdot}2H_2O$ in methanol dropwise. The mixture was stirred overnight in the dark. After evaporation to dryness, the solid residue was extracted with THF. Subsequent diffusion of diethyl ether into the concentrated THF solution gave the pale yellow crystals or solids.

2a. Yield: 21 mg, 23%. ^{1}H NMR (300 MHz, DMSO-d_6, 298 K): δ = 9.51 (s, 1 H, NH), 9.01 (s, 1 H, NH), 8.16 (d, J = 9 Hz, 2 H, aromatic ring), 7.66 (d, J = 9 Hz, 2 H, aromatic ring), 7.36 (d, J = 9 Hz, 2 H, aromatic ring), 7.19 (d, J = 9 Hz, 2 H, aromatic ring), 2.14−1.27 (m, 33 H, cyclohexyl). ^{31}P NMR (121 MHz, DMSO-d_6, 298 K): δ = 58.23. IR (KBr, cm^{-1}): ν = 3298 (N−H), 2054 (C≡C), 1715 (C═O). ESI-MS: m/z = 756 $[M - H]^-$. Anal. Calcd for $C_{33}H_{43}AuN_3O_3P$ (%): C, 52.31; H, 5.72; N, 5.55. Found: C, 52.02; H, 5.72; N, 5.36.

dx.doi.org/10.1021/ic202608r | Inorg. Chem. 2012, 51, 5099−5109

2b. Yield: 18 mg, 38%. ^{1}H NMR (300 MHz, DMSO-d_6, 298 K): δ = 9.08 (s, 1 H, NH), 8.81 (s, 1 H, NH), 7.62 (m, 4 H, aromatic ring), 7.32 (d, J = 7 Hz, 2 H, aromatic ring), 7.18 (d, J = 7 Hz, 2 H, aromatic ring), 2.10−1.27 (m, 33 H, cyclohexyl). ^{31}P NMR (121 MHz, DMSO-d_6, 298 K): δ = 58.21. ^{19}F NMR: (228 MHz, DMSO-d_6, 298 K): δ = −60.82. IR (KBr, cm^{-1}): ν = 3295 (N−H), 2104 (C≡C), 1714 (C═O). ESI-MS: m/z = 779 [M − H]$^-$. Anal. Calcd for $C_{34}H_{43}AuF_3N_2OP$ (%): C, 52.31; H, 5.55; N, 3.59. Found: C, 52.47; H, 5.60; N, 3.57.

2c. Yield: 19 mg, 20%. ^{1}H NMR (300 MHz, DMSO-d_6, 298 K): δ = 8.83 (s, 1 H, NH), 8.74 (s, 1 H, NH), 7.45 (d, J = 9 Hz, 2 H, aromatic ring), 7.31 (m, 4 H, aromatic ring), 7.16 (d, J = 9 Hz, 2 H, aromatic ring), 2.13−1.20 (m, 33 H, cyclohexyl). ^{31}P NMR (121 MHz, DMSO-d_6, 298 K): δ = 58.22. IR (KBr, cm^{-1}): ν = 3293 (N−H), 2104 (C≡C), 1708 (C═O). ESI-MS: m/z = 745 [M − H]$^-$. Anal. Calcd for $C_{33}H_{43}AuClN_2OP$ (%): C, 53.05; H, 5.80; N, 3.75. Found: C, 53.00; H, 5.81; N, 3.63.

2d. Yield: 36 mg, 42%. ^{1}H NMR (300 MHz, DMSO-d_6, 298 K): δ = 8.66 (s, 1 H, NH), 8.64 (s, 1 H, NH), 7.41 (d, J = 9 Hz, 2 H, aromatic ring), 7.32 (d, J = 9 Hz, 2 H, aromatic ring), 7.25 (dd, J_1 = 9 Hz, J_2 = 9 Hz, 2 H, aromatic ring), 7.16 (d, J = 9 Hz, 2 H, aromatic ring), 6.94 (dd, J_1 = 9 Hz, J_2 = 9 Hz, 1 H, aromatic ring), 2.14−1.27 (m, 33 H, cyclohexyl). ^{31}P NMR (121 MHz, DMSO-d_6, 298 K): δ = 58.22. IR (KBr, cm^{-1}): ν = 3273 (N−H), 2106 (C≡C), 1707 (C═O). ESI-MS: m/z = 711 [M − H]$^-$. Anal. Calcd for $C_{33}H_{44}AuN_2OP$ (%): C, 55.62; H, 6.22; N, 3.93. Found: C, 55.63; H, 6.28; N, 3.85.

2e. Yield: 67 mg, 76%. ^{1}H NMR (300 MHz, DMSO-d_6, 298 K): δ = 8.64 (s, 1 H, NH), 8.55 (s, 1 H, NH), 7.31 (d, J = 8 Hz, 2 H, aromatic ring), 7.30 (d, J = 8 Hz, 2 H, aromatic ring), 7.15 (d, J = 8 Hz, 2 H, aromatic ring), 7.06 (d, J = 8 Hz, 2 H, aromatic ring), 2.23 (s, 3 H, CH_3), 2.13−1.20 (m, 33 H, cyclohexyl). ^{31}P NMR (121 MHz, DMSO-d_6, 298 K): δ = 58.22. IR (KBr, cm^{-1}): ν = 3275 (N−H), 2106 (C≡C), 1707 (C═O). ESI-MS: m/z = 771 [M + EtOH − H]$^-$. Anal. Calcd for $C_{34}H_{46}AuN_2OP$ (%): C, 56.20; H, 6.38; N, 3.85. Found: C, 56.16; H, 6.32; N, 3.75.

2f. Yield: 25 mg, 27%. ^{1}H NMR (300 MHz, DMSO-d_6, 298 K): δ = 8.62 (s, 1 H, NH), 8.56 (s, 1 H, NH), 7.33 (d, J = 9 Hz, 2 H, aromatic ring), 7.32 (d, J = 9 Hz, 2 H, aromatic ring), 7.26 (d, J = 9 Hz, 2 H, aromatic ring), 7.15 (d, J = 9 Hz, 2 H, aromatic ring), 2.14−1.20 (m, 42H, cyclohexyl, and $C(CH_3)_3$). ^{31}P NMR (121 MHz, DMSO-d_6, 298 K): δ = 58.22. IR (KBr, cm^{-1}): ν = 3294 (N−H), 2108 (C≡C), 1709 (C═O). ESI-MS: m/z = 767 [M − H]$^-$. Anal. Calcd for $C_{37}H_{52}AuN_2OP$ (%): C, 57.81; H, 6.82; N, 3.64. Found: C, 57.51; H, 6.87; N, 3.46.

2g. Yield: 48 mg, 53%. ^{1}H NMR (300 MHz, DMSO-d_6, 298 K): δ = 8.58 (s, 1 H, NH), 8.45 (s, 1 H, NH), 7.32 (d, J = 9 Hz, 4 H, aromatic ring), 7.15 (d, J = 9 Hz, 2 H, aromatic ring), 6.84 (d, J = 9 Hz, 2 H, aromatic ring), 3.70 (s, 3 H, OCH_3), 2.11−1.31 (m, 33 H, cyclohexyl). ^{31}P NMR (121 MHz, DMSO-d_6, 298 K): δ = 58.22. IR (KBr, cm^{-1}): ν = 3275 (N−H), 2107 (C≡C), 1704 (C═O). ESI-MS: m/z = 741 [M − H]$^-$. Anal. Calcd for $C_{34}H_{46}AuN_2O_2P$ (%): C, 54.99; H, 6.24; N, 3.77. Found: C, 54.72; H, 6.19; N, 3.65.

3a. Yield: 35 mg, 39%. ^{1}H NMR (300 MHz, DMSO-d_6, 298 K): δ = 9.44 (s, 1 H, NH), 8.98 (s, 1 H, NH), 8.73 (d, J = 9 Hz, 2 H, aromatic ring), 7.62 (d, J = 9 Hz, 2 H, aromatic ring), 7.60−7.50 (m, 15 H, aromatic ring), 7.38 (d, J = 9 Hz, 2 H, aromatic ring), 7.24 (d, J = 9 Hz, 2 H, aromatic ring). ^{31}P NMR (121 MHz, DMSO-d_6, 298 K): δ = 42.72. IR (KBr, cm^{-1}): ν = 3300 (N−H), 2108 (C≡C), 1716 (C═O). ESI-MS: m/z = 739 [M]$^+$. Anal. Calcd for $C_{33}H_{25}AuN_3O_3P{\cdot}CH_3OH{\cdot}0.25CH_2Cl_2$ (%): C, 51.89; H, 3.75; N, 5.30. Found: C, 51.65; H, 3.69; N, 4.97.

3b. Yield: 19 mg, 22%. ^{1}H NMR (300 MHz, DMSO-d_6, 298 K): δ = 8.62 (s, 1 H, NH), 8.46 (s, 1 H, NH), 7.60−7.50 (m, 15 H, aromatic ring), 7.35 (d, J = 9 Hz, 2 H, aromatic ring), 7.31 (d, J = 9 Hz, 2 H, aromatic ring), 7.20 (d, J = 9 Hz, 2 H, aromatic ring), 6.85 (d, J = 9 Hz, 2 H, aromatic ring), 3.70 (s, 3 H, OCH_3). ^{31}P NMR (121 MHz, DMSO-d_6, 298 K): δ = 42.79. IR (KBr, cm^{-1}): ν = 3295 (N−H), 2114 (C≡C), 1647 (C═O). ESI-MS: m/z = 723 [M − H]$^-$. Anal. Calcd for $C_{34}H_{28}AuN_2O_2P$ (%): C, 56.36; H, 3.90; N, 3.87. Found: C, 56.16; H, 3.88; N, 3.80.

4a. Yield: 32 mg, 34%. ^{1}H NMR (300 MHz, DMSO-d_6, 298 K): δ = 8.69 (s, 1 H, NH), 8.65 (s, 1 H, NH), 7.45−7.11 (m, 20 H, aromatic ring), 6.95 (dd, J_1 = 8 Hz, J_2 = 8 Hz, 1 H, aromatic ring), 3.81 (s, 9 H, OCH_3). ^{31}P NMR (121 MHz, DMSO-d_6, 298 K): δ = 39.07. IR (KBr, cm^{-1}): ν = 3294 (N−H), 2046 (C≡C), 1714 (C═O). FAB-MS: m/z = 785 [M + H]$^+$. Anal. Calcd for $C_{36}H_{32}AuN_2O_4P$ (%): C, 55.11; H, 4.11; N, 3.57. Found: C, 54.83; H, 4.02; N, 3.55.

4b. Yield: 42 mg, 42%. ^{1}H NMR (300 MHz, DMSO-d_6, 298 K): δ = 8.63 (s, 1 H, NH), 8.47 (s, 1 H, NH), 7.45−7.11 (m, 18 H, aromatic ring), 6.85 (d, J = 9 Hz, 2 H, aromatic ring), 3.81 (s, 9 H, OCH_3), 3.70 (s, 3 H, OCH_3). ^{31}P NMR (121 MHz, DMSO-d_6, 298 K): δ = 39.05. IR (KBr, cm^{-1}): ν = 3284 (N−H), 2048 (C≡C), 1707 (C═O). FAB-MS: m/z = 815 [M + H]$^+$. Anal. Calcd for $C_{37}H_{34}AuN_2O_5P$ (%): C, 54.55; H, 4.21; N, 3.44. Found: C, 54.26; H, 4.09; N, 3.42.

Physical Measurements and Instrumentation. Chemical shifts (δ, ppm) were reported relative to tetramethylsilane for ^{1}H NMR, 85% H_3PO_4 for ^{31}P NMR, and NaF (δ = −122.4) for ^{19}F NMR on a Varian Mercury-Plus 300 spectrometer. Infrared spectra were recorded from KBr pellets in the range 400−4000 cm^{-1} on a Bruker-EQUINOX 55 FT-IR spectrometer. Electrospray ionization (ESI) mass spectra were recorded on a LCQ DECA XP quadrupole ion trap mass spectrometer. Fast atom bombardment (FAB) mass spectra were recorded on a Thermo MAT95XP high resolution mass spectrometer. Elemental analysis was performed on Elementar Vario EL elemental analyzer. Electronic absorption spectra were measured on a PGENERAL TU1901 UV−vis spectrophotometer. Emission spectra were obtained on a FLSP920 fluorescence spectrophotometer. Solution samples for emission spectra were degassed by four freeze−pump−thaw cycles.

Crystal Structure Determination. Crystals of **3a** and **4a** were grown by diffusion of diethyl ether into THF solution of the corresponding complexes. Selected single crystals of **3a** and **4a** were used for data collection on a Bruker SMART 1000 CCD diffractometer with graphite monochromatized Mo Kα radiation (λ = 0.710 73 Å) at 110 K. An empirical absorption correction was applied using the SADABS program.[33] The structures were solved by direct methods and refined by full-matrix least-squares based on F^2 using the SHELXTL program package.[34] CCDC 854038 and 854039 contain the supplementary crystallographic data for **3a** and **4a**, respectively. These data can be obtained free of charge via http://www.ccdc.cam.ac.uk/conts/retrieving.html, or from the Cambridge Crystallographic Data Center, 12 Union Road, Cambridge CB2 1EZ, U.K.; fax:(+44) 1223 336-033; or e-mail deposit@ccdc.cam.ac.uk.

Titrations and Job's Plots. For a typical UV−vis titration experiment, 1.5 μL aliquots of a tetra-*n*-butylammonium salt (1.98 × 10^{-3} mol dm^{-3} in THF or DMSO) were added into the 3 mL solution of the complex in THF or DMSO (1.98 × 10^{-5} mol dm^{-3} or 9.90 × 10^{-6} mol dm^{-3}) by a syringe, and the spectral changes were recorded by a PGENERAL TU1901 UV−vis spectrophotometer at 298 K. The volume changes after the addition of anions were kept less than 5% (150 μL). For a typical ^{1}H NMR titration experiment, 1 μL aliquots of a tetra-*n*-butylammonium salt (1.00 × 10^{-1} mol dm^{-3} in DMSO-d_6) were added into the 0.5 mL solution of the complex in DMSO-d_6 (5.00 × 10^{-3} mol dm^{-3} or 1.00 × 10^{-2} mol dm^{-3}) by a syringe, and the ^{1}H NMR spectral changes were recorded by a Varian Mercury-Plus 300 spectrometer at 298 K. The binding constant log K values were determined by nonlinear fitting using 1:1 model.[35] Job's plots were obtained from a series of solutions in which the fraction of the corresponding anions varied, keeping the total concentration (the complexes and anions) constant. The maxima of the plots indicated the binding stoichiometry of the complexes with anions.

RESULTS AND DISCUSSION

Syntheses and Characterization of Complexes 2a−2g, 3a−3b, and 4a−4b. Scheme 1 shows the synthetic route of mononuclear gold(I) acetylide complexes **2a−2g**, **3a−3b**, and **4a−4b**. The reaction of 4-[(trimethylsilyl)ethynyl]aniline with the corresponding isocyanate in dichloromethane gave acetylide ligands **1a−1g**. Mononuclear gold(I) acetylide complexes **2a−**

dx.doi.org/10.1021/ic202608r | Inorg. Chem. 2012, 51, 5099−5109

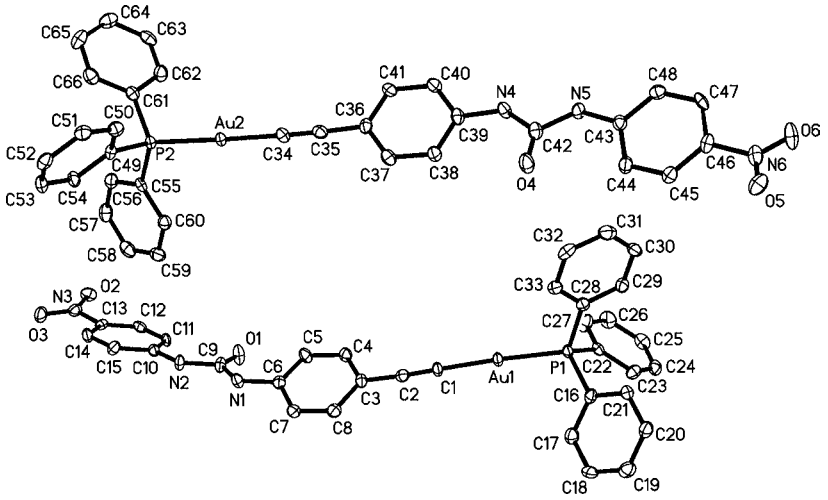

Figure 1. Perspective view of two independent molecules of **3a** with the atomic numbering scheme. Thermal ellipsoids are shown at the 50% probability level.

2g, **3a**−**3b**, and **4a**−**4b** were obtained by the reaction of R'_3PAuCl (R′ = cyclohexyl, phenyl, or 4-methoxyphenyl) with the corresponding acetylide ligands **1a**−**1g** in a molar ratio of 1:1 in the presence of an excess of KF in dichloromethane/methanol mixture at 298 K. The attempts to get other pure derivatives of gold(I) acetylide complexes with PR'_3 (R′ = phenyl or 4-methoxyphenyl) were not successful. All gold(I) acetylide complexes **2a**−**2g**, **3a**−**3b**, and **4a**−**4b** gave satisfactory elemental analyses and were characterized by FAB, ESI mass spectrometry and IR, ^{1}H, and ^{31}P NMR spectroscopy. They are air-stable in the solid state at 298 K.

The IR spectra of the gold(I) acetylide complexes **2a**−**2g**, **3a**−**3b**, and **4a**−**4b** reveal the bands at 3273−3300, 2046−2114, and 1647−1716 cm^{-1}, characteristic of the ν(N−H), ν(C≡C), and ν(C═O) stretches of acetylide ligands, respectively. The ^{1}H NMR spectra of complexes **2a**−**2g**, **3a**−**3b**, and **4a**−**4b** in DMSO-d_6 display two peaks at ca. δ 8.45−9.51 ppm, which are assigned as the resonances of the urea N−H of the acetylide ligand. For **2a**−**2g**, the chemical shifts of these peaks are in the following order: **2a** > **2b** > **2c** > **2d** ≥ **2e** ≈ **2f** ≥ **2g**, which is in line with the decreasing of the electron-withdrawing ability of R on the acetylide ligand. In addition, the chemical shifts at ca. δ 6.84−8.73 ppm are attributed to the resonances of the protons on the aromatic rings of the acetylide and arylphosphine ligands (or acetylide ligands only). The ^{31}P NMR spectra of the gold(I) acetylide complexes **2a**−**2g**, **3a**−**3b**, and **4a**−**4b** in DMSO-d_6 show a singlet at ca. δ 58.22, 42.72, and 39.07 ppm, respectively.

X-ray Crystal Structure Determination of 3a and 4a. The crystal structures of the gold(I) acetylide complexes **3a** and **4a** have been determined by X-ray crystallography, and their perspective drawings are shown in Figures 1 and 2, respectively. The crystallographic data as well as selected bond distances and angles are listed in Tables 1 and 2, respectively. For **4a**, the phenyl group and the amide nitrogen atom (N2 and N2A) on the urea moiety of the acetylide ligand are disordered over two positions with a 50:50 occupancy. The Au(I) coordination geometry in **3a** and **4a** are nearly linear with the P−Au−C angles 174.0(2)−177.51(15)°. The Au−P bond distances for **3a** and **4a** (2.2707(13)−2.281(2) Å) are similar to those reported for other gold(I) arylacetylide complexes with triphenylphosphine or tricyclohexylphosphine ligand.[30a,36]

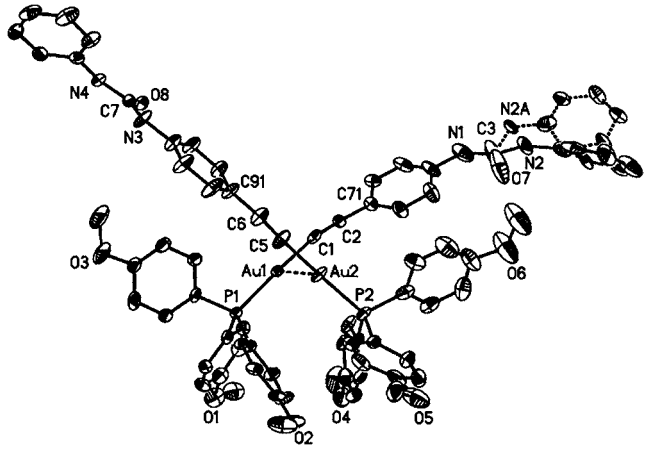

Figure 2. Perspective view of two independent molecules of **4a** with the atomic numbering scheme. Thermal ellipsoids are shown at the 30% probability level.

The Au−C (1.990(9)−2.041(9) Å) and C≡C (1.180(11)−1.206(7) Å) distances for **3a** and **4a** also resemble those in analogous gold(I) acetylide complexes.[30a,36] For **3a**, there are intermolecular $\pi\cdots\pi$ interactions (C(7A)···C(8AA) ~3.348 Å; C(8A)···C(7AA) ~3.348 Å; C(40A)···C(41B) ~3.365 Å; C(41A)···C(40B) ~3.365 Å) between two aromatic rings of acetylide ligands of two molecules (Figure S1, Supporting Information). In addition, intermolecular N−H···π(C≡C) interactions between the urea N−H and C≡C of two molecules of **3a** are observed (H(1AA)···C(1AA) ~2.926 Å; H(1AA)···C(2AA) ~2.646 Å; H(4BA)···C(34B) ~3.149 Å; H(4BA)···C(35B) ~2.895 Å; ∠N(4A)−H(4BA)−C(34B) ~123.58°; ∠N(1A)−H(1AA)−C(1AA) ~144.97°; ∠N(1A)−H(1AA)−C(2AA) ~136.64°; ∠N(4A)−H(4BA)−C(35B) ~119.52°) (Figure S1, Supporting Information). The oxygen atom of the nitro group and the nitrogen atom of the urea group show weak interactions with the gold atoms of **3a** (Au(1A)···O(5A) ~3.396 Å; Au(1A)···N(2AA) ~4.067 Å; Au(2A)···O(3A) ~3.363 Å; Au(2A)···N(5B) ~3.881 Å). There are intermolecular hydrogen bonding interactions between hydrogen atom (H5BB) of urea group and oxygen atom (O2A) of nitro group in the acetylide ligands of **3a** (Figure S1, Supporting Information). The hydrogen bonding parameters of

dx.doi.org/10.1021/ic202608r | Inorg. Chem. 2012, 51, 5099−5109

Table 1. Crystallographic Data for 3a and 4a

	3a	4a
formula	$C_{66}H_{50}Au_2N_6O_6P_2$	$C_{72}H_{64}Au_2N_4O_8P_2$
M (g/mol)	1478.99	1569.16
cryst syst	triclinic	triclinic
space group	$P\bar{1}$	$P\bar{1}$
a (Å)	12.4658(13)	11.878(2)
b (Å)	13.2527(14)	15.349(3)
c (Å)	17.6175(18)	20.733(4)
α (deg)	85.927(2)	101.74(3)
β (deg)	72.613(2)	97.22(3)
γ (deg)	87.304(2)	90.81(3)
V (Å^3)	2769.5(5)	3668.7(13)
Z	2	2
D_c (g cm^{-3})	1.774	1.422
T (K)	110(2)	110(2)
reflns collected	21 741	27 325
indep reflns	10 750	14 026
R_{int}	0.0236	0.0392
R,[a] R_w[b] [$I > 2\sigma(I)$]	0.0264, 0.0804	0.0592, 0.1598
GOF	1.114	1.051

[a] $R = \sum(|F_o| - |F_c|)/\sum|F_o|$. [b] $R_w = [\sum w(|F_o| - |F_c|)^2/\sum w|F_o|^2]^{1/2}$.

3a are listed in Table S1 (Supporting Information). For 4a, there are intermolecular N−H···π(C≡C) interactions between the urea N−H and C≡C of two molecules (H(1A)···C(5B) ~2.424 Å; H(1A)···C(6B) ~2.682 Å; ∠N(1)−H(1A)−C(5B) ~166.10°; ∠N(1)−H(1A)−C(6B) ~162.91°; H(3A)···C(1A) ~2.382 Å; H(3A)···C(2A) ~2.921 Å; ∠N(3)−H(3A)−C(1A) ~164.69°; ∠N(3)−H(3A)−C(2A) ~146.08°; H(4A)···C(1A) ~2.444 Å; H(4A)···C(2A) ~2.668 Å; ∠N(4)−H(4A)−C(1A) ~160.06°; ∠N(4)−H(4A)−C(2A) ~149.67°) (Figure S2, Supporting Information). The nearest gold···gold distance (Au(1)···Au(2)) is 3.0145(9) Å, indicating the existence of weak gold···gold interaction in 4a.

Electronic Absorption and Emission Spectroscopy of Complexes 2a−2g, 3a−3b, and 4a−4b. The photophysical data for complexes 2a−2g, 3a−3b, and 4a−4b are summarized in Table 3. For comparison, the photophysical data of the corresponding free acetylide ligands 1a−1g are listed in Table S2 (Supporting Information). Figure S3 (Supporting Information) shows the electronic absorption spectrum of 2a in THF at 298 K. The absorption peak maxima of 2a appear at 263, 276, 288, 301, and 345 nm, which are red-shifted compared to those of the free acetylide ligand 1a. The red-shift could come from the orbital interaction between the acetylide ligand and Au 5d orbitals.[36f] The spacings of adjacent absorption maxima of 2a at 263−301 nm are ca. 1500 and 1800 cm^{-1}. Thus, the absorption bands of complex 2a at 263−301 nm are assigned as the $\pi \rightarrow \pi^*$ transitions of the acetylide ligands. The low-energy absorption band of 2a at 345 nm could be due to the charge-transfer transition from the amide to the NO_2 group of the acetylide ligand.[18b] The absorption spectra of non-nitro-derivatives 2b−2g, 3b, and 4a−4b in THF at 298 K exhibit one shoulder (ca. 264 nm) and three bands (ca. 279, 293, and 310 nm) (Figures S4−S6, Supporting Information). The vibrational spacings are in two kinds of wavenumbers, ca. 1700 and 2000 cm^{-1}, which are ascribed to ν(C═O) and ν(C≡C), respectively. These absorption bands are assigned to $^1(\pi\pi^*)$ transition involving carbonyl and acetylenic units of the acetylide ligand.

Excitation of complexes 2a−2g, 3b, and 4a−4b both in the solid state and in THF solution at $\lambda > 290$ nm produces luminescence in the visible light regime. Figure 3 displays the emission spectrum of 2d in the solid state at 298 K (for the emission spectra of 2a, 2b, and 2g in the solid state at 298 K, see Figures S7 and S8 (Supporting Information)). It shows vibronic fine structures with the progressional spacings of four different frequencies, ca. 1100, 1600, 1700, and 2000 cm^{-1}, which are attributed to the phenyl ring deformation, symmetric phenyl ring stretch, C═O stretching, and C≡C stretching frequencies of the ground state, respectively. Similar spacings were observed for other gold(I) acetylide complexes.[30a] Except for 3a, the gold(I) acetylide complexes studied in this paper in THF at 298 K exhibit blue-green emission. Two emission maxima are observed at ca. 443 and 476 nm with the vibrational progressional spacing of approximately 1600 cm^{-1} (for the emission spectra of 2a−2g, 3b, and 4a−4b in THF at 298 K, see Figures S9 and S10 (Supporting Information)). The observed large Stokes shifts together with long lifetimes in the microsecond range of the emission suggest the origin of the emission has triplet parentage. Thus, the lowest-lying emissive state of complexes 2b−2g, 3b, and 4a−4b is assigned as the $^3(\pi\pi^*)$ excited state of the acetylide ligand, which is promoted through the spin−orbit coupling due to the introduction of gold atom.[30a,b] The broad emission band of 2a in the solid state

Table 2. Selected Bond Lengths (Å) and Angles (deg) for 3a and 4a

3a		4a	
Au(1)−C(1)	2.003(5)	Au(1)−C(1)	2.041(9)
Au(2)−C(34)	2.000(5)	Au(2)−C(5)	1.990(9)
Au(1)−P(1)	2.2804(13)	Au(1)−P(1)	2.281(2)
Au(2)−P(2)	2.2707(13)	Au(2)−P(2)	2.273(2)
C(1)−C(2)	1.203(7)	C(1)−C(2)	1.180(11)
C(34)−C(35)	1.206(7)	C(5)−C(6)	1.202(12)
C(9)−O(1)	1.212(6)	C(3)−O(7)	1.10(3)
C(42)−O(4)	1.204(6)	C(7)−O(8)	1.230(9)
P(1)−Au(1)−C(1)	176.78(14)	Au(1)···Au(2)	3.0145(9)
P(2)−Au(2)−C(34)	177.51(15)	P(1)−Au(1)−C(1)	174.0(2)
Au(1)−C(1)−C(2)	174.4(5)	P(2)−Au(2)−C(5)	175.4(3)
Au(2)−C(34)−C(35)	176.1(5)	Au(1)−C(1)−C(2)	169.3(7)
C(1)−C(2)−C(3)	176.8(5)	Au(2)−C(5)−C(6)	176.6(11)
C(34)−C(35)−C(36)	175.5(6)	C(1)−C(2)−C(71)	175.2(9)
		C(5)−C(6)−C(91)	173.4(11)

dx.doi.org/10.1021/ic202608r | Inorg. Chem. 2012, 51, 5099−5109

Table 3. Photophysical Data of Complexes 2a−2g, 3a−3b, and 4a−4b

complex	medium (298 K)	λ_{abs}/nm (ε/dm^3 mol^{-1} cm^{-1})	λ_{em}/nm (τ_0/μs)
2a	THF	263 (sh, 12 500), 276 (23 300), 288 (30 800), 301 (28 600), 345 (24 000)	443 (max, 6.5), 474
	solid		525 (<0.1)
2b	THF	266 (sh, 18 700), 280 (sh, 35 300), 295 (60 400), 311 (63 200)	443 (max, 7.9), 475
	solid		443, 479 (max, 18.6), 505, 528
2c	THF	264 (sh, 20 000), 279 (36 600), 293 (58 900), 310 (58 700)	443 (max, 7.7), 476
	solid		440, 479 (max, 15.2), 530 (sh)
2d	THF	264 (sh, 22 300), 279 (28 500), 293 (54 400), 310 (55 200)	444 (max, 21.5), 474
	solid		443, 479 (max, 20.3), 505, 518, 529
2e	THF	266 (sh, 17 400), 279 (33 400), 293 (54 900), 310 (55 400)	443 (max, 7.8), 475
	solid		440, 481 (max, 11.9), 532 (sh)
2f	THF	265 (sh, 16 300), 280 (sh, 32 400), 293 (51 800), 310 (51 400)	444 (max, 7.6), 475
	solid		444, 489 (max, 7.6)
2g	THF	265 (sh, 16 800), 280 (sh, 33 600), 293 (56 400), 310 (58 300)	443 (max, 19.9), 475
	solid		440, 480 (max, 16.1), 505, 517, 529
3a	THF	268 (18 800), 276 (22 400), 292 (28 000), 305 (27 900), 342 (27 100)	no emission
	solid		no emission
3b	THF	268 (24 000), 276 (sh, 26 600), 284 (sh, 30 100), 299 (45 900), 315 (46 500)	444 (max, 8.6), 475
	solid		440, 473, 485 (max, 36.1), 510(sh)
4a	THF	279 (38 600), 296 (48 400), 313 (49 700)	444 (max, 7.6), 474
	solid		448, 495 (max, 15.9)
4b	THF	279 (sh, 37 400), 297(52 100), 314 (54 000)	443 (max, 19.4), 476
	solid		449, 503 (max, 13.2)

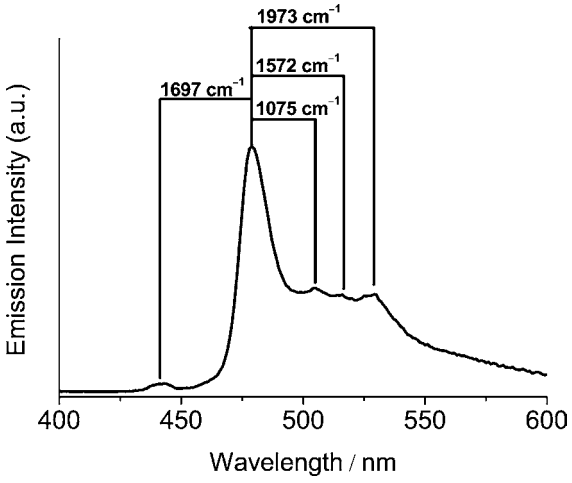

Figure 3. Emission spectrum of **2d** in the solid state at 298 K (λ_{ex} = 293 nm).

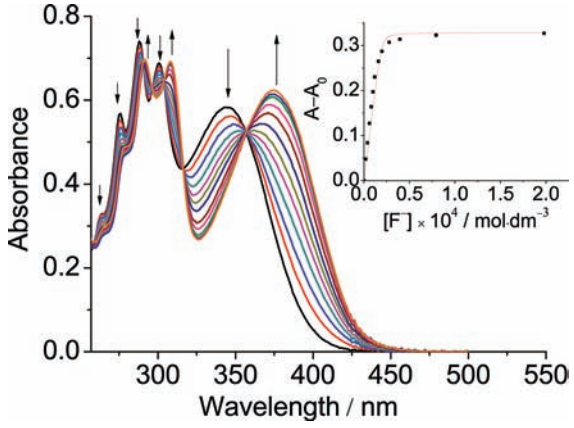

Figure 4. UV−vis spectral changes of **2a** (1.98×10^{-5} mol dm^{-3}) in THF upon addition of F$^-$. Insert: a plot of the absorbance change at 375 nm as a function of the concentration of F$^-$ and its theoretical fit for the 1:1 binding of complex **2a** with F$^-$.

centered at 525 nm (Figure S7, Supporting Information) could be ascribed to the charge transfer from NO_2 to amide of the acetylide ligand. For the gold(I) acetylide complexes studied in this paper, except the nitro-derivatives **2a** and **3a**, the substituent R on the acetylide ligand as well as the type of phosphine ligand have little effect on the electronic absorption and emission spectra.

Anion Binding Properties of Complexes 2a−2g, 3a−3b, and 4a−4b. *Anion Binding of Complexes in THF.* The anion-sensing abilities of **2a−2g**, **3a−3b**, and **4a−4b** in THF have been studied by UV−vis titration experiments. Because $NBu_4H_2PO_4$ and NBu_4HSO_4 have limited solubility in THF, the investigations toward $H_2PO_4^-$ and HSO_4^- were not carried out. Figure 4 shows the UV−vis spectral changes of **2a** upon addition of F$^-$ in THF at 298 K. The absorbance of the absorption bands of **2a** at 263, 276, 288, 301, and 345 nm decreases gradually, while the new absorption bands at 292, 308, and 375 nm appear gradually upon addition of F$^-$. Well-defined isosbestic points are observed at 290, 296, 304, 316, and 357 nm, indicating that only two species coexist during the titration equilibrium and suggesting the possible formation of anion−complex adduct.

The UV−vis spectral changes of gradual addition of F$^-$ into **2b−2g**, **3b**, **4a**, and **4b** in THF are similar: three gradually decreasing bands (ca. 279, 295, and 310 nm) and two newly formed absorption bands (ca. 305 and 319 nm). There are three well-defined isosbestic points at ca. 299, 310, and 313 nm (see Figures S11−S14 (Supporting Information) for the UV−vis spectral changes of **2b**, **2d**, **2e**, and **2g** upon addition of F$^-$ in THF, respectively). The UV−vis spectral changes of nitro-derivative **3a** upon addition of F$^-$ in THF are similar to those of **2a**, but only one isosbestic point at 357 nm is observed (Figure S15, Supporting Information).

dx.doi.org/10.1021/ic202608r | *Inorg. Chem.* 2012, 51, 5099−5109

Figure 5 shows the Job's plots of **2b**, **2c**, and **2g** with F^- in THF (for **2a**, **2d**, **2e**, and **2f**, see Figures S16–S19 (Supporting Information), respectively). The absorbance reaches maximum at ca. 0.5, indicating the 1:1 binding between F^- and **2a–2g** in THF. Using the 1:1 binding model, the log *K* values of **2a–2g**, **3a–3b**, and **4a–4b** toward F^- are determined and listed in Table 4. For the complexes **2a–2g** with Cy_3P ligand, their log *K* values with F^- are in the following order: R = NO_2 (**2a**) > CF_3 (**2b**) ≥ Cl (**2c**) > H (**2d**) > CH_3 (**2e**) ≈ ^{t}Bu (**2f**) ≥ OCH_3 (**2g**), which is in line with the decreasing of the electron-withdrawing ability of the substituent R on the acetylide ligand of **2a–2g**. This could be rationalized by the fact that the electron-withdrawing substituent R on the acetylide ligand of **2a–2g** would increase the acidity of urea N–H and strengthen the hydrogen bond interactions between the urea N–H of the complex and F^-. The trend of the average chemical shifts of urea N–H of **2a–2g** in DMSO-d_6 is R = NO_2 (**2a**) > CF_3 (**2b**) > Cl (**2c**) > H (**2d**) ≥ CH_3 (**2e**) ≈ ^{t}Bu (**2f**) ≥ OCH_3 (**2g**), revealing the order of the acidity of urea N–H of **2a–2g**.

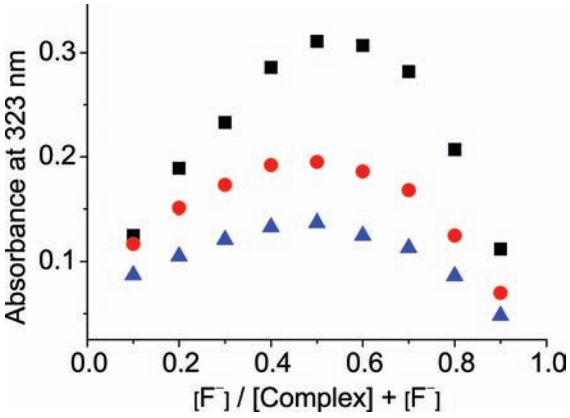

Figure 5. Job's plots of complexes **2b** (■), **2c** (●), and **2g** (▲) with F^- in THF ([complex] + [F^-] = 1.98 × 10^{-5} mol dm^{-3}).

For complexes with triphenylphosphine or tris(4-methoxyphenyl)phosphine ligand, **3a**, **3b**, **4a**, and **4b**, their log *K* values with F^- are in the order **3a** > **3b**; **4a** > **4b**, showing the same substituent (R) effect on the log *K* value as previously observed in **2a–2g** (Table 4). For the complexes with same acetylide ligand but different phosphine ligands, their log *K* values toward F^- show the following order: **2a** ≥ **3a**; **2g** > **3b** ≈ **4b**; **2d** > **4a**. This result indicates that the change of R′ on the phosphine ligand has a little effect on log *K* value.

The binding abilities of **2a–2g**, **3a–3b**, and **4a–4b** toward other anions (OAc^-, Cl^-, Br^-, and NO_3^-) have also been investigated in THF at 298 K (Table 4). The UV–vis spectral changes of **2b** toward anions (OAc^-, Cl^-, Br^-, and NO_3^-) in THF are similar to those of **2b** toward F^- in THF. Figure 6 shows the UV–vis spectral changes of **2b** in THF upon addition of OAc^- (for the UV–vis spectral changes of **2b** toward Cl^-, Br^-, and NO_3^-, see Figures S20–S22 (Supporting Information), respectively). A well-defined isosbestic point at 299 nm is found, illustrating the coexistence of complex and corresponding anion-complex adduct. The log *K* values of **2b** in THF toward anions are in the following order: F^- > OAc^- ≈ Cl^- > Br^- > NO_3^-. Figure S23 (Supporting Information) shows the plots of absorbance change of **2b** upon addition of various anions (for **2c** and **3a**, see Figures S24 and S25 (Supporting Information), respectively). The similar order is also found in **2c–2g** and **3a** toward different anions (Table 4).

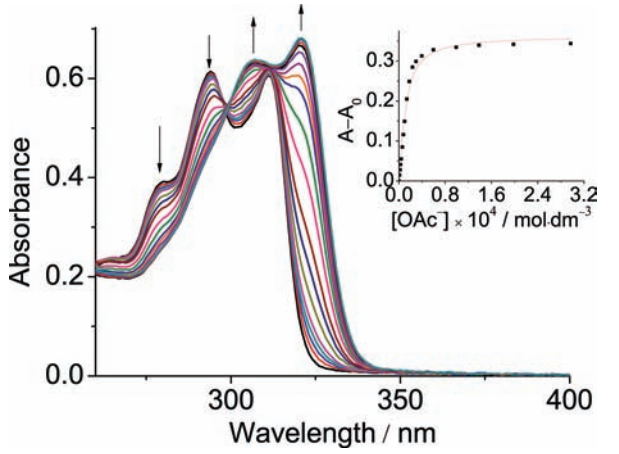

Figure 6. UV–vis spectral changes of **2b** in THF (9.90 × 10^{-6} mol dm^{-3}) upon addition of OAc^-. Insert: a plot of the absorbance change at 321 nm as a function of the concentration of OAc^- and its theoretical fit for the 1:1 binding of complex **2b** with OAc^-.

The anion-binding constants of the acetylide ligands, HC≡CC_6H_4-4-NHC(O)NHC_6H_4-4-R (R = NO_2 (**5a**), CF_3 (**5b**), Cl

Table 4. Binding Constants of 2a–2g, 3a–3b, and 4a–4b for Anions in THF[a]

	log *K*				
complex	F^-	OAc^-	Cl^-	Br^-	NO_3^-
2a	6.44 ± 0.13	5.92 ± 0.06	*b*	*b*	*b*
2b	5.76 ± 0.10	5.18 ± 0.06	5.23 ± 0.02	4.86 ± 0.03	4.75 ± 0.06
2c	5.57 ± 0.11	4.99 ± 0.02	4.95 ± 0.02	4.83 ± 0.03	4.55 ± 0.05
2d	4.97 ± 0.02	4.81 ± 0.02	4.81 ± 0.04	4.73 ± 0.02	4.32 ± 0.04
2e	4.75 ± 0.03	4.78 ± 0.01	4.46 ± 0.01	4.25 ± 0.06	4.22 ± 0.05
2f	4.74 ± 0.03	4.52 ± 0.05	4.48 ± 0.01	3.98 ± 0.05	4.08 ± 0.04
2g	4.70 ± 0.02	4.55 ± 0.04	4.23 ± 0.03	3.78 ± 0.02	4.06 ± 0.04
3a	6.20 ± 0.08	6.24 ± 0.06	5.88 ± 0.10	4.93 ± 0.04	5.68 ± 0.23
3b	4.57 ± 0.03	4.50 ± 0.03	*b*	*b*	4.13 ± 0.02
4a	4.74 ± 0.02	4.69 ± 0.01	*b*	*b*	4.12 ± 0.07
4b	4.54 ± 0.01	4.60 ± 0.01	*b*	*b*	3.86 ± 0.09

[a]Binding constants were determined by 1:1 model using nonlinear fitting methods. [b]Spectral changes were not suitable for accurate measurement of binding constant.

dx.doi.org/10.1021/ic202608r | *Inorg. Chem.* 2012, 51, 5099–5109

(**5c**), H (**5d**), CH_3 (**5e**), ^{t}Bu (**5f**), OCH_3 (**5g**)), in THF have also been determined to compare with those of gold(I) acetylide complexes **2a**−**2g** (Table S3, Supporting Information). For the same acetylide ligand (**5a**−**5g**), the log *K* values toward anions in THF show the selectivity in the following order: $OAc^- > F^- > Cl^- > Br^- > NO_3^-$. For the same anion, the log *K* values of the acetylide ligands **5a**−**5g** in THF are in the following order: **5a** > **5b** ≥ **5c** > **5d** ≈ **5f** ≈ **5g** > **5e**. In general, the acetylide ligands **5a**−**5g** show smaller anion-binding constants than their corresponding gold(I) acetylide complexes **2a**−**2g** in THF.

The hydrogen bond competition investigations have been carried out. Figure 7 shows the UV−vis spectral changes of **2a**

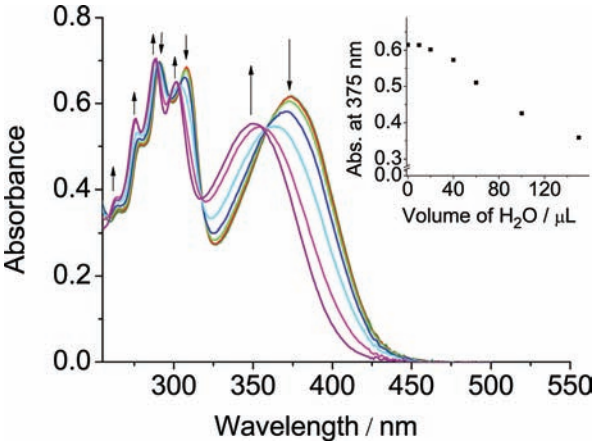

Figure 7. UV−vis spectral changes of **2a** with 10 equiv of F^- in THF (1.98×10^{-5} mol dm^{-3}) upon addition of H_2O. Insert: a plot of the absorbance at 375 nm as a function of the volume of H_2O.

with 10 equiv of F^- in THF upon addition of H_2O. Upon addition of H_2O, the UV−vis spectrum is gradually backed to that of **2a** in THF. The addition of other protic solvent, such as MeOH or EtOH, into **2a** with 10 equiv of F^- in THF produces similar spectral changes. This could be ascribed to the formation of hydrogen bonds between the protic solvent (water or alcohols) and F^-, preventing F^- from forming hydrogen bonds with **2a**.

Anion Binding of Complexes in DMSO. In order to investigate the effect of polarity of solvent on the binding abilities of complexes toward anions, UV−vis and ^{1}H NMR titration experiments of **2a**, **2b**, **2d**, and **2g** toward anions in DMSO and DMSO-d_6 have been carried out. Figure 8 shows the UV−vis spectral changes of **2a** in DMSO upon addition of F^- at 298 K. The absorbance of the absorption bands at 275, 288, 303, and 356 nm decreases, while the absorbance of the absorption band at 324 and 485 nm gradually increases and the solution gradually becomes orange-yellow after 1 equiv of F^- is added. The appearance of the low-energy absorption band at 485 nm, which does not appear in the titration of **2a** with F^- in THF, is ascribed to the deprotonation of the urea N−H of **2a**. Upon addition of F^- into **2b** in DMSO (Figure S26, Supporting Information), the additional low-energy absorption band (compared with the spectral changes of **2b** with F^- in THF) at ca. 352 nm forms, and the color of the solution becomes light yellow. On the contrary, there is no obvious low-energy absorption band at λ > 345 nm upon addition of F^- into the DMSO solution of **2d** or **2g**, and their UV−vis spectral changes are similar to those of **2d** or **2g** with F^- in THF (Figures S27

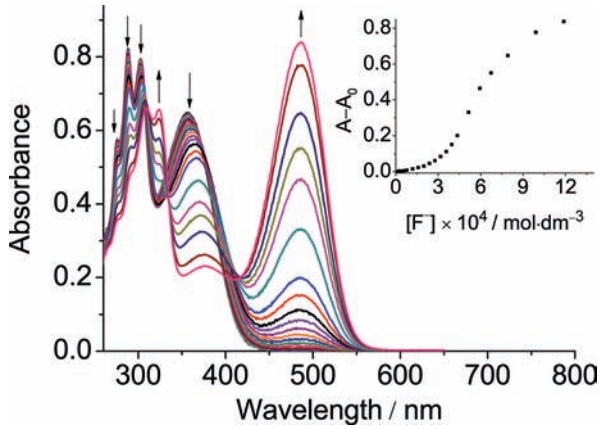

Figure 8. UV−vis spectral changes of **2a** (1.98×10^{-5} mol dm^{-3}) in DMSO upon addition of F^-. Insert: a plot of the absorbance at 485 nm as a function of the concentration of F^-.

and S28, Supporting Information, respectively). This could be rationalized by the fact that the electron-withdrawing substituent R (NO_2 or CF_3) on the acetylide ligands of **2a** or **2b** could increase the acidity of urea N−H and facilitate the deprotonation process of corresponding urea N−H in DMSO.[10b−e]

Unlike the UV−vis titration spectra of **2a** with F^- in DMSO, the UV−vis spectral changes of **2a** toward OAc^- in DMSO are similar to those in THF and the color of the solution becomes light yellow upon addition of OAc^- (Figure S29, Supporting Information). For comparison, the UV−vis spectra and colors of **2a** with 50 equiv of F^- or OAc^- in THF as well as in DMSO are shown in Figure 9. The UV−vis spectra of **2a** with 50 equiv of F^- in THF and **2a** with 50 equiv of OAc^- in THF as well as

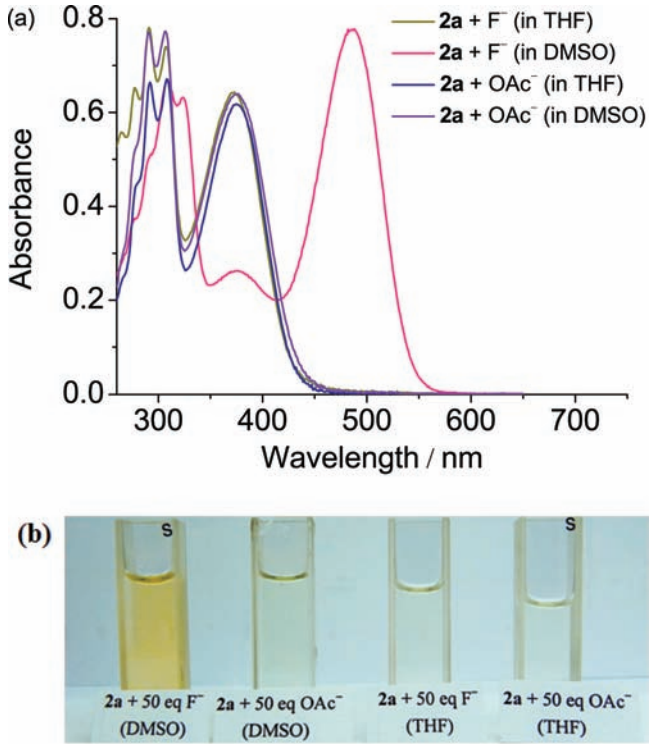

Figure 9. UV−vis spectra (a) and colors (b) of **2a** (1.98×10^{-5} mol dm^{-3}) in THF or DMSO in the presence of 50 equiv of F^- or OAc^-.

dx.doi.org/10.1021/ic202608r | Inorg. Chem. 2012, 51, 5099−5109

DMSO are almost the same, while an additional low-energy absorption band appears at 485 nm for **2a** with 50 equiv of F^- in DMSO. Addition of $H_2PO_4^-$ into **2a** in DMSO provides the UV−vis spectral changes similar to those of **2a** with OAc^- in DMSO (Figure S30, Supporting Information). Thus, the dramatic color change of **2a** is only observed toward F^- in DMSO. This solvent-dependent and selective color change of **2a** toward F^- provides an access of naked eye detection of F^-.

The interactions of **2a**, **2b**, **2d**, and **2g** with anions (F^- and OAc^-) in DMSO-d_6 have also been investigated by ^{1}H NMR titration experiments. The ^{1}H NMR spectral changes of **2a** upon addition of OAc^- in DMSO-d_6 are shown in Figure 10.

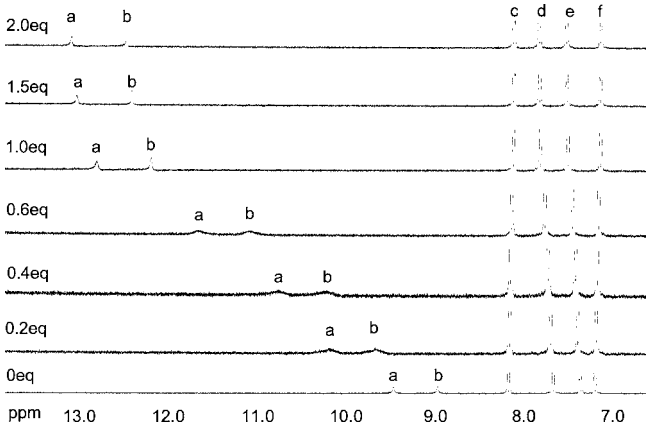

Figure 10. ^{1}H NMR spectral changes of **2a** in DMSO-d_6 (5 mmol dm^{-3}) upon addition of OAc^-.

The significant downfield shift of the signals of urea N−H (H_a and H_b) is observed upon addition of OAc^- from 0 to 2 equiv, and these chemical shifts have a little change after addition of 2 equiv of OAc^-, suggesting the formation of hydrogen bonds between the urea N−H of **2a** and OAc^-. The signals of aromatic protons of **2a** (H_c−H_f) show the slight shift upon addition of OAc^- from 0 to 2 equiv. The slight upfield shift of H_c and H_f could be ascribed to the increase of shielding effect which is introduced by the enhancement of electron density of aromatic ring by the through-bond propagation.[10b−e] In contrast, the slight downfield shift of H_d and H_e is ascribed to the polarization effect of the C−H bond that is introduced by the through-space effect.[10b−e]

Figure 11 shows the ^{1}H NMR spectral changes of **2a** upon addition of F^- in DMSO-d_6, which are quite different from those of **2a** with OAc^- in DMSO-d_6. Upon addition of F^- into **2a** in DMSO-d_6, the signals of two urea protons (H_a and H_b) of **2a** disappear, while the distinct triplet centered at 16.08 ppm (J_{HF} = 120 Hz), which is assigned as the signal of HF_2^-,[37] appears upon addition of 5 equiv of F^- (Figure S31, Supporting Information). The signals of aromatic protons H_c−H_f show little shift when less than 1 equiv of F^- is added. Upon addition of more than 1 equiv of F^- into **2a** in DMSO-d_6, signals of H_c, H_d, and H_f show dramatic upfield shift, which could be ascribed to the drastic enhancement of shielding effect resulting from the increased electron density of aromatic ring through the increased through-bond negative charge delocalization that caused by the deprotonation process of urea N−H.[10b−e] The downfield shift of H_e could be ascribed to the domination of the polarization effect of the C−H bond.[10b−e] The ^{1}H NMR spectral changes of **2a** upon addition of F^- in THF-d_8 are similar to those of **2a** with OAc^- in DMSO-d_6 (Figure S32, Supporting Information). The ^{19}F NMR spectra of **2a** upon addition of 5 equiv of F^- in DMSO-d_6 and THF-d_8 are shown in Figure S33 (Supporting Information). The HF_2^- signal appearing at −142.7 ppm (doublet, J_{HF} = 120 Hz)[10e,37] for the former also supports the ascription of the deprotonation process of the urea N−H of **2a** in DMSO-d_6.

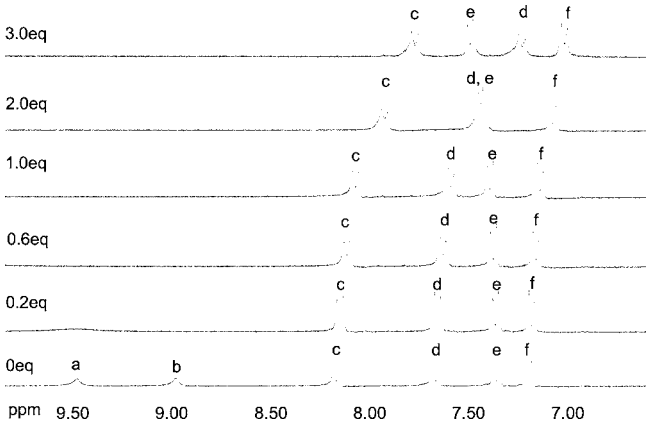

Figure 11. ^{1}H NMR spectral changes of **2a** (10 mmol dm^{-3}) upon addition of F^- in DMSO-d_6.

The ^{1}H NMR spectral changes of **2b** with F^- in DMSO-d_6 are similar to those of **2a** with F^- in DMSO-d_6 (Figure S34, Supporting Information). On the contrary, spectral changes of **2d** or **2g** with F^- in DMSO-d_6 are similar to those of **2a** with OAc^- in DMSO-d_6 (Figures S35 and S36, Supporting Information, respectively). These results indicate that the deprotonation process of the urea N−H is present in the interaction of **2a** and **2b** with F^- in DMSO-d_6.

The binding constants of **2a**, **2b**, **2d**, and **2g** with OAc^- as well as $H_2PO_4^-$ in DMSO were determined from the UV−vis titration experiments. Their log K values are listed in Table S4 (Supporting Information). The log K values of the same complex with various anions are in the following order: $OAc^- \geq H_2PO_4^-$, which is in line with the decrease of the basicity of anions. The binding constants of different complexes with the same anion (OAc^- or $H_2PO_4^-$) are in the following order: R = NO_2 (**2a**) > CF_3 (**2b**) > H (**2d**) ≥ OCH_3 (**2g**). The same order is also observed for these complexes with the same anion in THF and suggests the same effect of the electron-withdrawing ability of the substituent R on the acetylide ligand of complexes on log K values. The log K values of **2a**, **2b**, **2d**, and **2g** with OAc^- in DMSO are comparatively smaller than those in THF, and the difference among these log K values in DMSO is small. This suggests that in this case the less polar solvent THF exhibits a more promotive and differentiating effect on log K values than DMSO.

■ CONCLUSION

Urea based gold(I) acetylide complexes **2a**−**2g**, **3a**−**3b**, and **4a**−**4b** have been synthesized and characterized. Complexes **2b**−**2g**, **3b**, and **4a**−**4b** both in the solid state and in degassed THF solution produce intense luminescence, which is assigned to come from the $^3(\pi\pi^*)$ excited state of the acetylide ligands of the complexes. In THF, the substituent R on the acetylide ligand of complexes has influence on the anion-binding ability, with the log K values of **2a**−**2g** toward the same anion in the following order: R = NO_2 (**2a**) > CF_3 (**2b**) ≥ Cl (**2c**) > H (**2d**) > CH_3 (**2e**) ≈ ^{t}Bu (**2f**) ≥ OCH_3 (**2g**). On the other hand, the substituent R′ on phosphine ligand of complexes has little effect

dx.doi.org/10.1021/ic202608r | Inorg. Chem. 2012, 51, 5099−5109

on log K values with the same anion. The less polar solvent THF shows a more promotive and differentiating effect on log K values than DMSO. In DMSO, **2a** shows the selective color change toward F^-, and this is ascribed to the deprotonation of urea N−H of the acetylide ligand of **2a**. The solvent-dependent and selective color change of **2a** toward F^- provides access for naked eye detection of F^-.

■ ASSOCIATED CONTENT

Supporting Information

X-ray crystallographic files in CIF format for complexes **3a** and **4a**. Additional figures and tables. This material is available free of charge via the Internet at http://pubs.acs.org.

■ AUTHOR INFORMATION

Corresponding Author

*Phone: +86-20-84110062. Fax: +86-20-84112245. E-mail: zhaoxy@mail.sysu.edu.cn.

Notes

The authors declare no competing financial interest.

■ ACKNOWLEDGMENTS

We acknowledge financial support from the National Natural Science Foundation of China (20671097, 20971131, 20901084, and J1103305), the Doctoral Fund of Ministry of Education of China for New Scholar (200805581015), the Natural Science Foundation of Guangdong Province (10151027501000048), the Undergraduate Innovative Experiment Program of Guangdong Province (1055811083), and Sun Yat-Sen University. We also thank the editor and reviewers for helpful comments and suggestions.

■ REFERENCES

(1) Park, C. H.; Simmons, H. E. *J. Am. Chem. Soc.* **1968**, *90*, 2431−2431.

(2) (a) Xu, Z.; Chen, X.; Kim, H. N.; Yoon, J. *Chem. Soc. Rev.* **2010**, *39*, 127−137. (b) Kubik, S. *Chem. Soc. Rev.* **2010**, *39*, 3648−3663.

(3) (a) Gale, P. A. *Acc. Chem. Res.* **2011**, *44*, 216−226. (b) Kim, S. K.; Lee, D. H.; Hong, J. I.; Yoon, J. *Acc. Chem. Res.* **2009**, *42*, 23−31. (c) Li, X.; Wu, Y. D.; Yang, D. *Acc. Chem. Res.* **2008**, *41*, 1428−1438. (d) Davis, A. P. *Coord. Chem. Rev.* **2006**, *250*, 2939−2951.

(4) (a) Davis, A. P.; Brotherhood, P. R. *Chem. Soc. Rev.* **2010**, *39*, 3633−3647. (b) Smith, B. D.; O'Neil, E. J. *Coord. Chem. Rev.* **2006**, *250*, 3068−3080. (c) Beer, P. D.; Gale, P. A. *Angew. Chem., Int. Ed.* **2001**, *40*, 486−516.

(5) Gamez, P.; Mooibroek, T. J.; Teat, S. J.; Reedijk, J. *Acc. Chem. Res.* **2007**, *40*, 435−444.

(6) Metrangolo, P.; Cavallo, G.; Pilati, T.; Resnati, G.; Sansotera, M.; Terraneo, G. *Chem. Soc. Rev.* **2010**, *39*, 3772−3783.

(7) (a) Li, A. F.; Wang, J. H.; Wang, F.; Jiang, Y. B. *Chem. Soc. Rev.* **2010**, *39*, 3729−3745. (b) Fabbrizzi, L.; Amendola, V.; Mosca, L. *Chem. Soc. Rev.* **2010**, *39*, 3889−3915.

(8) (a) Bowman-James, K.; Kang, S. O.; Hossain, M. A. *Coord. Chem. Rev.* **2006**, *250*, 3038−3052. (b) Bondy, C. R.; Loeb, S. J. *Coord. Chem. Rev.* **2003**, *240*, 77−99.

(9) Best, M. D.; Tobey, S. L.; Anslyn, E. V. *Coord. Chem. Rev.* **2003**, *240*, 3−15.

(10) (a) Amendola, V.; Fabbrizzi, L.; Mosca, L.; Schmidtchen, F. P. *Chem.—Eur. J.* **2011**, *17*, 5972−5981. (b) Gomez, D. E.; Fabbrizzi, L.; Licchelli, M.; Monzani, E. *Org. Biomol. Chem.* **2005**, *3*, 1495−1500. (c) Esteban-Gomez, D.; Fabbrizzi, L.; Liechelli, M. *J. Org. Chem.* **2005**, *70*, 5717−5720. (d) Boiocchi, M.; Del Boca, L.; Esteban-Gomez, D.; Fabbrizzi, L.; Licchelli, M.; Monzani, E. *Chem.—Eur. J.* **2005**, *11*, 3097−3104. (e) Boiocchi, M.; Del Boca, L.; Gomez, D. E.; Fabbrizzi, L.; Licchelli, M.; Monzani, E. *J. Am. Chem. Soc.* **2004**, *126*, 16507−16514.

(11) (a) Duke, R. M.; Gunnlaugsson, T. *Tetrahedron Lett.* **2011**, *52*, 1503−1505. (b) dos Santos, C. M. G.; Boyle, E. M.; De Solis, S.; Kruger, P. E.; Gunnlaugsson, T. *Chem. Commun.* **2011**, *47*, 12176−12178. (c) Duke, R. M.; Gunnlaugsson, T. *Tetrahedron Lett.* **2010**, *51*, 5402−5405. (d) Ali, H. D. P.; Kruger, P. E.; Gunnlaugsson, T. *New J. Chem.* **2008**, *32*, 1153−1161. (e) Quinlan, E.; Matthews, S. E.; Gunnlaugsson, T. *J. Org. Chem.* **2007**, *72*, 7497−7503. (f) Duke, R. M.; Gunnlaugsson, T. *Tetrahedron Lett.* **2007**, *48*, 8043−8047. (g) Quinlan, E.; Matthews, S. E.; Gunnlaugsson, T. *Tetrahedron Lett.* **2006**, *47*, 9333−9338. (h) Gunnlaugsson, T.; Davis, A. P.; O'Brien, J. E.; Glynn, M. *Org. Biomol. Chem.* **2005**, *3*, 48−56.

(12) (a) Busschaert, N.; Wenzel, M.; Light, M. E.; Iglesias-Hernandez, P.; Perez-Tomas, R.; Gale, P. A. *J. Am. Chem. Soc.* **2011**, *133*, 14136−14148. (b) Edwards, P. R.; Hiscock, J. R.; Gale, P. A.; Light, M. E. *Org. Biomol. Chem.* **2010**, *8*, 100−106. (c) Caltagirone, C.; Hiscock, J. R.; Hursthouse, M. B.; Light, M. E.; Gale, P. A. *Chem.—Eur. J.* **2008**, *14*, 10236−10243. (d) Caltagirone, C.; Gale, P. A.; Hiscock, J. R.; Brooks, S. J.; Hursthouse, M. B.; Light, M. E. *Chem. Commun.* **2008**, 3007−3009. (e) Caltagirone, C.; Bates, G. W.; Gale, P. A.; Light, M. E. *Chem. Commun.* **2008**, 61−63. (f) Brooks, S. L.; Garcia-Garrido, S. E.; Light, M. E.; Cole, P. A.; Gale, P. A. *Chem.—Eur. J.* **2007**, *13*, 3320−3329.

(13) (a) Carroll, C. N.; Coombs, B. A.; McClintock, S. P.; Johnson Ii, C. A.; Berryman, O. B.; Johnson, D. W.; Haley, M. M. *Chem. Commun.* **2011**, *47*, 5539−5541. (b) Ahmed, N.; Geronimo, I.; Hwang, I. C.; Singh, N. J.; Kim, K. S. *Chem.—Eur. J.* **2011**, *17*, 8542−8548. (c) Jia, C.; Wu, B.; Li, S.; Yang, Z.; Zhao, Q.; Liang, J.; Li, Q. S.; Yang, X. J. *Chem. Commun.* **2010**, *46*, 5376−5378. (d) Meshcheryakov, D.; Bohmer, V.; Bolte, M.; Hubscher-Bruder, V.; Arnaud-Neu, F. *Chem.—Eur. J.* **2009**, *15*, 4811−4881. (e) Schazmann, B.; Alhashimy, N.; Diamond, D. *J. Am. Chem. Soc.* **2006**, *128*, 8607−8614. (f) Bryantsev, V. S.; Hay, B. P. *J. Am. Chem. Soc.* **2006**, *128*, 2035−2042. (g) Hay, B. P.; Firman, T. K.; Moyer, B. A. *J. Am. Chem. Soc.* **2005**, *127*, 1810−1819. (h) Cho, E. J.; Moon, J. W.; Ko, S. W.; Lee, J. Y.; Kim, S. K.; Yoon, J.; Nam, K. C. *J. Am. Chem. Soc.* **2003**, *125*, 12376−12377.

(14) Steed, J. W. *Chem. Soc. Rev.* **2009**, *38*, 506−519.

(15) (a) Cormode, D. P.; Evans, A. J.; Davis, J. J.; Beer, P. D. *Dalton. Trans.* **2010**, *39*, 6532−6541. (b) Molina, P.; Tárraga, A.; Caballero, A. *Eur. J. Inorg. Chem.* **2008**, *2008*, 3401−3417. (c) Oton, F.; Tarraga, A.; Espinosa, A.; Velasco, M. D.; Molina, P. *Dalton. Trans.* **2006**, 3685−3692. (d) Oton, F.; Tarraga, A.; Velasco, M. D.; Espinosa, A.; Molina, P. *Chem. Commun.* **2004**, 1658−1659. (e) Miyaji, H.; Collinson, S. R.; Prokes, I.; Tucker, J. H. R. *Chem. Commun.* **2003**, 64−65. (f) Alonso, B.; Casado, C. M.; Cuadrado, I.; Moran, M.; Kaifer, A. E. *Chem. Commun.* **2002**, 1778−1779.

(16) (a) Ghosh, A.; Verma, S.; Ganguly, B.; Ghosh, H. N.; Das, A. *Eur. J. Inorg. Chem.* **2009**, *2009*, 2496−2507. (b) Ghosh, A.; Ganguly, B.; Das, A. *Inorg. Chem.* **2007**, *46*, 9912−9918.

(17) (a) dos Santos, C. M. G.; Gunnlaugsson, T. *Dalton. Trans.* **2009**, 4712−4721. (b) dos Santos, C. M. G.; Fernandez, P. B.; Plush, S. E.; Leonard, J. P.; Gunnlaugsson, T. *Chem. Commun.* **2007**, 3389−3391.

(18) (a) He, X.; Yam, V. W. W. *Inorg. Chem.* **2010**, *49*, 2273−2279. (b) He, X.; Herranz, F.; Cheng, E. C. C.; Vilar, R.; Yam, V. W. W. *Chem.—Eur. J.* **2010**, *16*, 9123−9131. (c) He, X.; Zhu, N.; Yam, V. W. W. *Dalton. Trans.* **2011**, *40*, 9703−9710.

(19) (a) Yam, V. W. W.; Cheng, E. C. C. *Chem. Soc. Rev.* **2008**, *37*, 1806−1813. (b) Yam, V. W. W.; Cheng, E. C. C. *Top. Curr. Chem.* **2007**, *281*, 269−309.

(20) Abdou, H. E.; Mohamed, A. A.; Fackler, J. P.; Burini, A.; Galassi, R.; Lopez-de-Luzuriaga, J. M.; Olmos, M. E. *Coord. Chem. Rev.* **2009**, *253*, 1661−1669.

(21) (a) Ott, I. *Coord. Chem. Rev.* **2009**, *253*, 1670−1681. (b) Navarro, M. *Coord. Chem. Rev.* **2009**, *253*, 1619−1626. (c) Bindoli, A.; Rigobello, M. P.; Scutari, G.; Gabbiani, C.; Casini, A.; Messori, L. *Coord. Chem. Rev.* **2009**, *253*, 1692−1707.

(22) (a) Nolan, S. P. *Acc. Chem. Res.* **2011**, *44*, 91−100. (b) Li, Z.; Brouwer, C.; He, C. *Chem. Rev.* **2008**, *108*, 3239−3265. (c) Hashmi, A. S. K. *Chem. Rev.* **2007**, *107*, 3180−3211.
(23) (a) Evans, R. C.; Douglas, P.; Winscom, C. J. *Coord. Chem. Rev.* **2006**, *250*, 2093−2126. (b) Zhou, G. J.; Wong, W. Y. *Chem. Soc. Rev.* **2011**, *40*, 2541−2566.
(24) (a) He, X.; Yam, V. W. W. *Coord. Chem. Rev.* **2011**, *255*, 2111−2123. (b) He, X.; Zhu, N.; Yam, V. W. W. *Organometallics.* **2009**, *28*, 3621−3624. (c) He, X.; Lam, W. H.; Zhu, N.; Yam, V. W. W. *Chem.—Eur. J.* **2009**, *15*, 8842−8851. (d) He, X.; Cheng, E. C. C.; Zhu, N.; Yam, V. W. W. *Chem. Commun.* **2009**, 4016−4018. (e) Tang, H. S.; Zhu, N.; Yam, V. W. W. *Organometallics.* **2007**, *26*, 22−25. (f) Lu, X. X.; Li, C. K.; Cheng, E. C. C.; Zhu, N.; Yam, V. W. W. *Inorg. Chem.* **2004**, *43*, 2225−2227. (g) Yam, V. W. W.; Yip, S. K.; Yuan, L. H.; Cheung, K. L.; Zhu, N.; Cheung, K. K. *Organometallics.* **2003**, *22*, 2630−2637. (h) Yam, V. W. W.; Cheung, K. L.; Yuan, L. H.; Wong, K. M. C.; Cheung, K. K. *Chem. Commun.* **2000**, 1513−1514.
(25) (a) Yam, V. W. W.; Wong, K. M. C. *Top. Curr. Chem.* **2005**, *257*, 1−32. (b) Yam, V. W. W. *Acc. Chem. Res.* **2002**, *35*, 555−563.
(26) Long, N. J.; Williams, C. K. *Angew. Chem., Int. Ed.* **2003**, *42*, 2586−2617.
(27) (a) Powell, C. E.; Humphrey, M. G. *Coord. Chem. Rev.* **2004**, *248*, 725−756. (b) Lima, J. C.; Rodríguez, L. *Chem. Soc. Rev.* **2011**, *40*, 5442−5456.
(28) Fan, Y.; Zhu, Y. M.; Dai, F. R.; Zhang, L. Y.; Chen, Z. N. *Dalton. Trans.* **2007**, 3885−3892.
(29) (a) Fillaut, J. L.; Andries, J.; Perruchon, J.; Desvergne, J. P.; Toupet, L.; Fadel, L.; Zouchoune, B.; Saillard, J. Y. *Inorg. Chem.* **2007**, *46*, 5922−5932. (b) Fillaut, J. L.; Andries, J.; Toupet, L.; Desvergne, J. P. *Chem. Commun.* **2005**, 2924−2926.
(30) (a) Chao, H. Y.; Lu, W.; Li, Y.; Chan, M. C. W.; Che, C. M.; Cheung, K. K.; Zhu, N. *J. Am. Chem. Soc.* **2002**, *124*, 14696−14706. (b) Che, C. M.; Chao, H. Y.; Miskowski, V. M.; Li, Y.; Cheung, K. K. *J. Am. Chem. Soc.* **2001**, *123*, 4985−4991. (c) Chao, H. Y.; Wu, L.; Su, B. C.; Feng, X. L. *Inorg. Chem. Commun.* **2011**, *14*, 122−124. (d) Zhang, M.; Su, B. C.; Li, C. L.; Shen, Y.; Lam, C. K.; Feng, X. L.; Chao, H. Y. *J. Organomet. Chem.* **2011**, *696*, 2654−2659.
(31) Serwinski, P. R.; Lahti, P. M. *Org. Lett.* **2003**, *5*, 2099−2102.
(32) Al-sa'ady, A. K.; Mcauliffe, C. A.; Parish, R. V.; Sandbank, J. A. *Inorg. Synth.* **1985**, *23*, 191−194.
(33) Sheldrick, G. M. *SADABS: Program for Empirical Absorption Correction of Area Detector Data*; University of Göttingen: Göttingen, Germany, 1996.
(34) Sheldrick, G. M. *SHELXTL: Structure Determination Software Programs*; Bruker Analytical X-ray Systems Inc.: Madison, WI, 1997.
(35) Bourson, J.; Pouget, J.; Valeur, B. *J. Phys. Chem.* **1993**, *97*, 4552−4557.
(36) (a) Chow, A. L. F.; So, M. H.; Lu, W.; Zhu, N.; Che, C. M. *Chem.—Asian J.* **2011**, *6*, 544−553. (b) Lin, Y.; Yin, J.; Yuan, J.; Hu, M.; Li, Z.; Yu, G. A.; Liu, S. H. *Organometallics.* **2010**, *29*, 2808−2814. (c) Xu, H. B.; Zhang, L. Y.; Ni, J.; Chao, H. Y.; Chen, Z. N. *Inorg. Chem.* **2008**, *47*, 10744−10752. (d) Yip, S. K.; Cheng, E. C. C.; Yuan, L. H.; Zhu, N.; Yam, V. W. W. *Angew. Chem., Int. Ed.* **2004**, *43*, 4954−4957. (e) Yam, V. W. W.; Lo, K. K. W.; Wong, K. M. C. *J. Organomet. Chem.* **1999**, *578*, 3−30. (f) Irwin, M, J.; Vittal, J, J.; Puddephatt, R, J. *Organometallics.* **1997**, *16*, 3541−3547.
(37) (a) Descalzo, A. B.; Rurack, K.; Weisshoff, H.; Martínez-Máñez, R.; Marcos, M. D.; Amorós, P.; Hoffmann, K.; Soto, J. *J. Am. Chem. Soc.* **2004**, *127*, 184−200. (b) Jia, C.; Wu, B.; Liang, J.; Huang, X.; Yang, X. J. *J. Fluoresc.* **2010**, *20*, 291−297.